The ARGeo geophysical model of the Tendaho geothermal field, Ethiopia

Egidio Armadillo[1], Daniele Rizzello[2], Jim Stimac[3], Meseret Zemedkun[4], Solomon Kebede[5], Andarge Mengiste[5]

[1]University of Genoa, [2]Tellus sas, [3]Stimac Geothermal Consulting, [4]UNEP, [5]Geological Survey of Ethiopia

egidio@dipteris.unige.it

Keywords: Magnetotellurics, Gravity, Magnetics, Tendaho Graben.

ABSTRACT

The Dubti and Ayrobera geothermal systems are located in the Tendaho Graben (Afar region, Ethiopia). As part of the ARGeo 2014 program, we have integrated the available geophysical data set with new measurements. The new residual magnetic anomaly map has been used to map the younger (<0.78 Ma) normal polarity basalt distribution and infer the location of the main rift axis hindered by sediments. The bedrock surface obtained by 3D inversion of the gravity residual anomaly gives a first order insight on the geometry of the graben. The graben sediments are marked by a shallow electrical conductor, with exceptionally low resistivities <1 Ohm m**,** mainly ascribed to low temperature clay alteration. Local resistivity variations are due to basalt interlayerings and coarser components. Resistivity 2D inversion models show a deep conductive anomaly that has been previously mapped and interpreted as an upper crustal fracture zone that lies above a 15 km wide area of partial melt . The new magnetotelluric data acquired to the South of Dubti manifestations indicate that the conductive anomaly is shallower and more intense to the South and approximately centred below the anomalous stripe of recent dikes/intrusions.

1. INTRODUCTION

The African Rift Geothermal Development Facility Program (ARGeo) originated in 2003 to assist development of the East African Rift geothermal resources that represent one of the largest untapped geothermal potential worldwide (Teklemariam Zemedkun, 2011). As part of the ARGeo 2014 program, the United Nations Environment Program (UNEP) founded the "Geothermal Resource Assessment of Tendaho Geothermal Field in Ethiopia" project, proposed by the Geothermal Division of the Geological Survey of Ethiopia (GSE). All the accessible geoscientific data have been reviewed and new MT and TDEM data have been acquired in some essential areas, with the aim of identifying target sites for deep exploratory wells and minimize the risk of exploration (Stimac et al., 2014).

The Tendaho geothermal field is made by two close manifestations areas, namely Dubti and Ayrobera (Fig. 1). In the area of Dubti and Ayrobera, extensive geo-scientific investigations were carried out starting from the 1960's and six exploratory wells at different depths were drilled in the 1990's (Aquater, 1996). A shallow secondary reservoir was identified by drilling at Dubti in the depth range 200-500 m. However, its areal extent is uncertain and additional concerns about the possible environmental impact have prevented its exploitation up to now. The deep primary reservoir is more attractive for the associated reduced environmental risk and the expected higher potential, with estimated temperature in the range 220-270 °C (Abdurahman, 2011). However, its location and extension, expected in some tectonically fractured portion of the Afar Stratoids basalts close to the Dubti manifestations (Aquater, 1996; Battistelli et al., 2002; Stimac et al., 2014), is still uncertain as well as its relationships with the Ayrobera manifestations.

A preliminary review of the ARGeo Tendaho project results can be found in Stimac et al. (2014). Here we focus on models and interpretations of the whole available geophysical data set. In order to get a deeper insight in the Dubti and Ayrobera geothermal systems and relationships, we have i) re-processed the potential field data obtaining new 2D and 3D models and ii) integrated the existing available MT data set with new measurements in key sectors.

2. GEOLOGICAL SETTING

The Tendaho Graben (TG) is the largest depression in central Afar (Fig. 1). It is a NW-SE trending extensional feature related to the complex geotectonic framework of the Afar triple junction, where three propagators join together: the Main Ethiopian Rift, the Red Sea Rift and the Aden Rift.

Acocella et al. (2008) speculate that two main offset and non-overlapping spreading axes have been active, in part simultaneously, within TG in the last ~1.8 Ma, in a context of decreasing volcanic and tectonic activity. The relevant rifting episode forming TG may have been induced by the generation and rise of a significant amount of magma, leading to the repeated fissural emission of significant volumes of Stratoids, between ~1.8 and ~0.6 Ma. According to this model, from ~0.2 Ma volcanic activity was restricted to selected spots (Kurub, Manda Gargori and Dama Ale), while the new focus of spreading, with moderate extension rates and eruptive volumes, migrated to the Manda Hararo Rift (MHR) segment that constitutes the currently active axial zone of the TG (Fig. 1). In this setting, the Kurub, Manda Gargori and Dama Ale volcanic system is interpreted to result from the gradual termination of the former Tendaho

Rift, rather than being the southern continuation of the MHR (Fig. 1).

In the TG normal faulting is dominant (Fig. 1), although some sinistral strike slip is present (Abbate et al., 1995; Acocella et al., 2008). The amount of rift-perpendicular extension across TG has been estimated by Acocella et al. (2008) who gave a stretching factor B=1.1, that implies a total extension of about 5 km at an extension rate of ~3.6 mm/yr for the last ~1.4 Ma, one to two orders of magnitude larger than that of the nearby grabens (Acton et al., 2000). Extension gave rise to about 1600 m of vertical displacement verified by drilling of the Afar Stratoid sequence.

The bedrock of the TG mainly comprises Stratoid deposits, which generally young toward the central part of the graben (Lahitte et al., 2003; Kidane et al., 2003). The infill of TG, overlying the Stratoids, consists of volcanic and sedimentary deposits, among which are, to the NW, the youngest basaltic deposits (0.22– 0.03 Ma) of the axial part of MHR. The northernmost part of MHR, outside the study area, underwent a major rifting episode in 2005, associated with the emplacement of a dike 60 km long and up to 8 m wide.

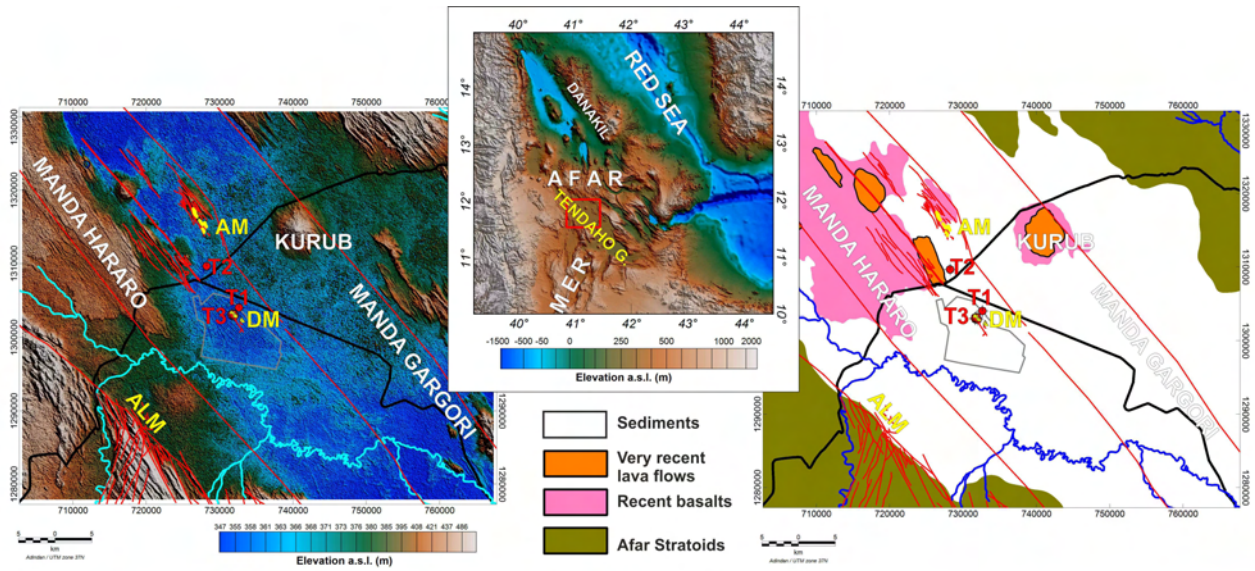

Figure 1 - Center: the Tendaho Graben location in Afar. Left: the survey area. AM, DM, ALM: Ayrobera, Dubti and Alalo Bed manifestations; TD1-TD3: location of deep exploratory wells. Right: simplified geological map from Abbate et al. (1995), Aquater (1996) and Stimac et al. (2014).

3. THE GRAVIMETRIC SURVEY

The gravimetric data set is made by 2377 stations of the GSE/Aquater 1979/80, 1996 and 2004 surveys (Bekele, 2012). The measurement points are shown as small black dots in Fig. 2. The data set is made very sparse lines and high density sampling along the lines; moreover the levelling errors between intersecting lines may seriously bias the anomaly pattern. We have therefore decided to down weight the short wavelength component in the residual Bouguer anomaly map by upward continuation up to 1000 m (Fig. 2). We have identified four main positive (high) domains labelled H1 – H4 and two negative (low) domains labelled L1 – L2. The H1 domain is located in the middle of the region and includes the Ayrobera area. L1 trends parallel to the Graben strike and separates H1 and H2 highs. L2 area is a wide minimum comprising the Dubti plantations. The Dubti manifestations are situated at the northern edge of L2. The shown linear trends were identified by total horizontal derivative (gradient) of the terracing operator

We have mapped the bedrock surface by 3D inversion of the free air gravimetric data with Geosoft GM-SYS 3D software. We have assigned to the Afar stratoids a density of 2750 kg/m3 and to the sedimentary infill 2200 kg/m3 (Bridges, 2011). We have then assumed as starting model a flat bedrock surface at -600 m a.s.l. The software has then altered the starting bedrock surface in order to fit the measured gravimetric data. The surface we have obtained must be considered as an *ideal* surface (Fig. 2, right). It would be coincident with the true bedrock surface of the Afar stratoids if *i*) the sediments and the bedrock would have the constant assigned density contrast all over the area and if *ii*) the plane starting surface would be a good mean approximation of the true one. The first hypothesis could be largely violated by the presence of the basalt interlayering in the sedimentary sequence. Here the surface traces the upper limit of the basalt rich sedimentary layer rather than the Afar Stratoids bedrock that can be considerably below. This is probably the case of the North West sector (gravity high H1 in Fig. 2), where the estimated bedrock surface appears strongly biased by the presence of recent basalt interlayerings in the sediments.

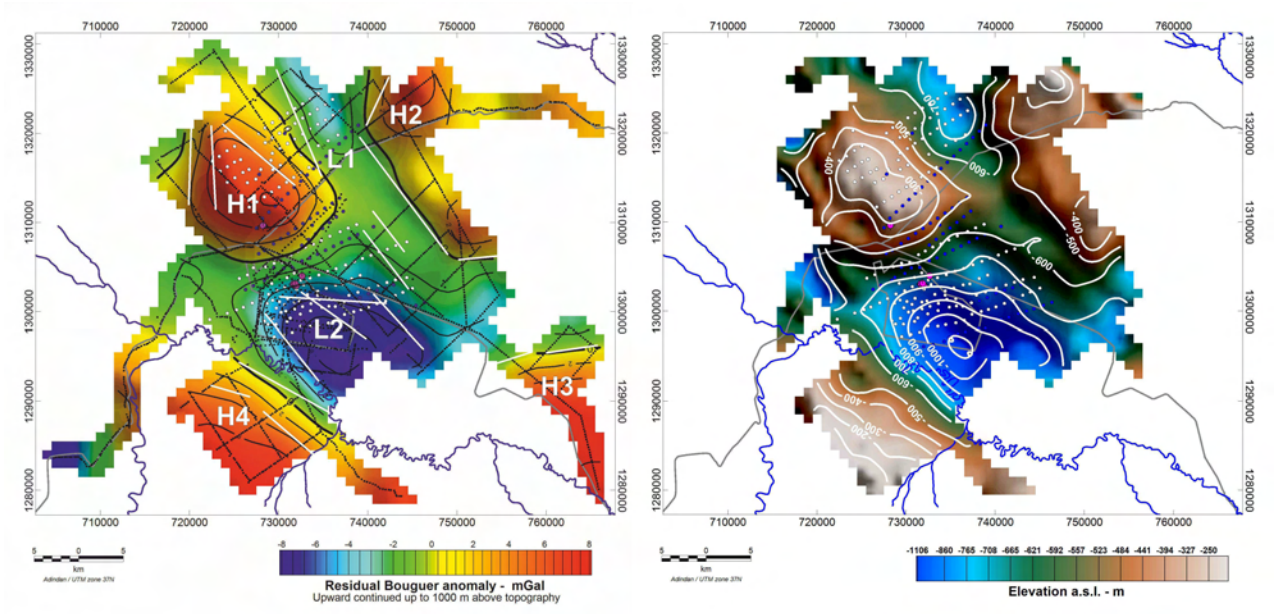

Figure 2 - Left: residual Bouguer anomaly map upward continued to 1000 m above topography. The 0 mGal contour line (heavy black line) helps to individuate four main positive (high) domains labelled H1 – H4 and two negative (low) domains labelled L1 – L2. White lines are the linear trends interpreted from the total horizontal derivative of the terracing operator. Right: bedrock surface derived from 3D inversion of the gravity free air anomaly. The estimated bedrock surface is potentially biased by the presence of basalt interlayerings that alter the density contrast between sediments and bedrock here assumed to be 550 kg/m3 constant over the whole area.

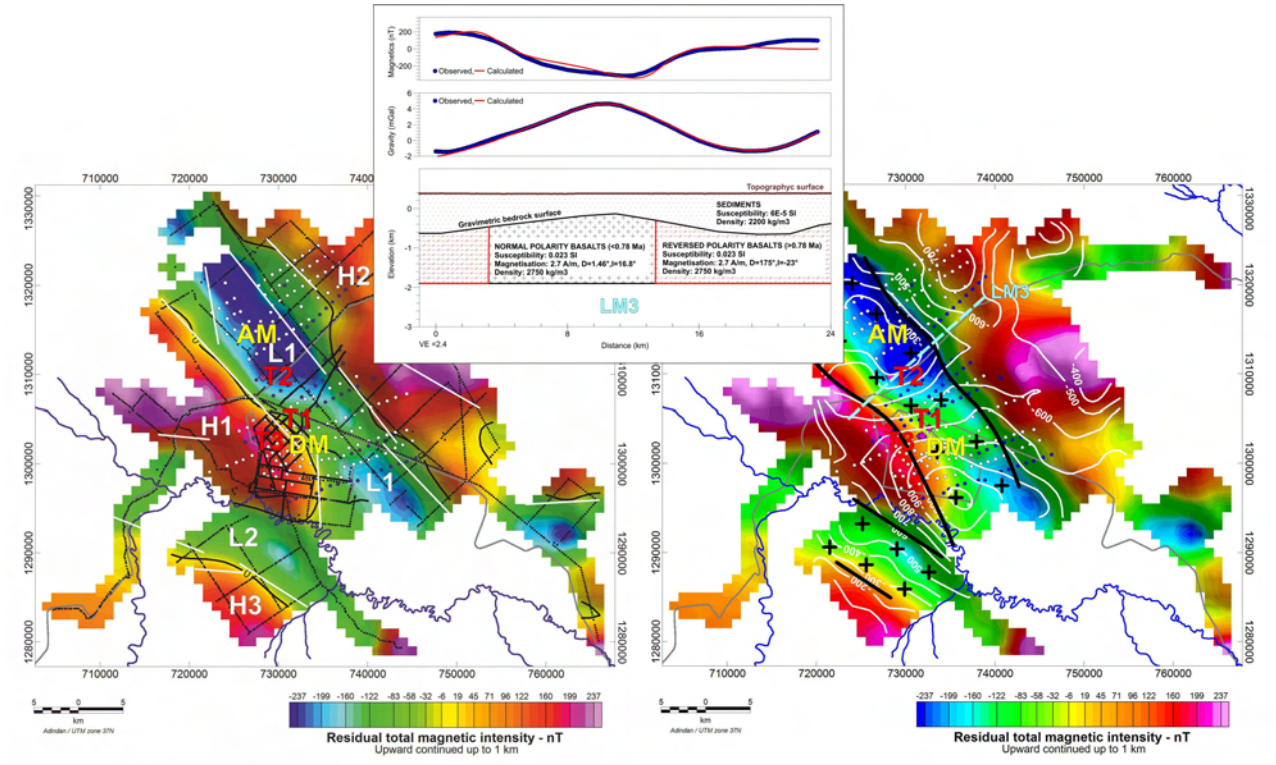

Figure 3 - Left: residual magnetic intensity anomaly map upward continued up to 1000 m above topography. The 0 nT contour line (heavy black line) helps to individuate three main positive (high) domains labelled H1 – H3 and two negative (low) domains labelled L1 – L2. White lines are the linear trends interpreted from the total horizontal derivative of the terracing operator. Center: simplified magnetic and gravimetric 2D forward model for profile LM3. Right: regions (heavy black plus signs) of dominantly normal-polarity intrusions and/or diking as derived from the 2D modelling. White lines indicate the contour of the depth a.s.l. of the "gravity bedrock surface"

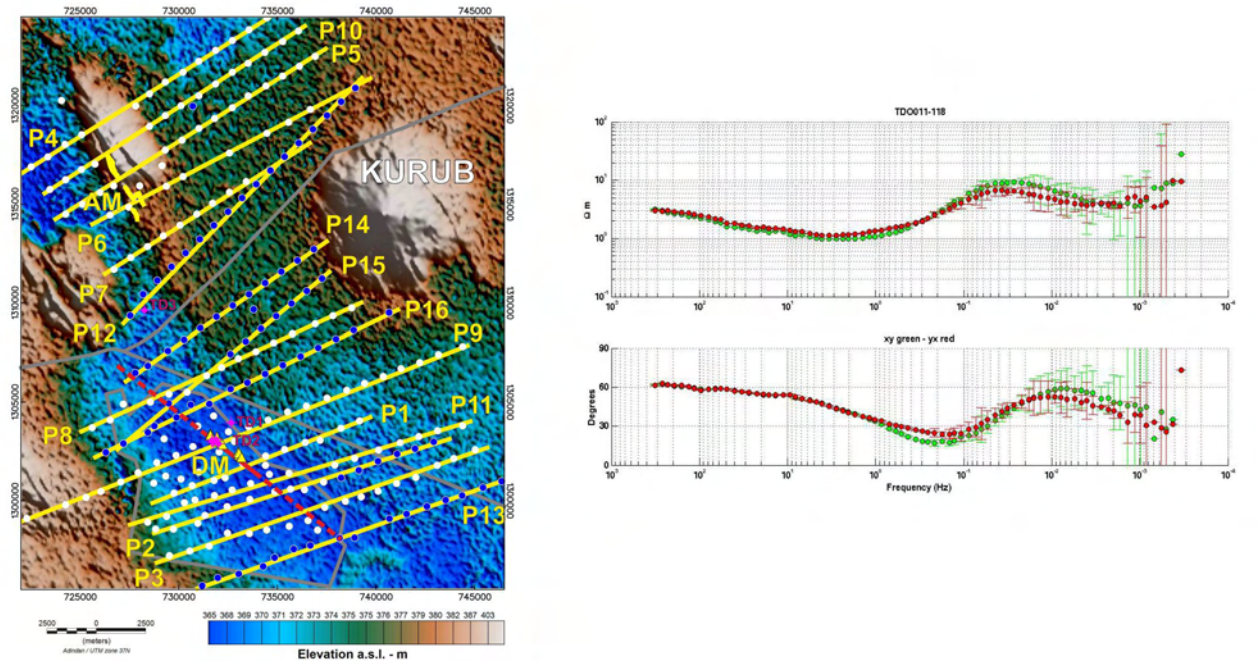

Figure 4 - Left: Location of the MT stations and profiles; the blue dots indicate the new ARGeo 84 MT stations acquired by GSE in 2014; locations of the exploratory wells TD1-TD3 are marked by magenta crosses; the Dubti fault (as reported by Aquater, 1996) and its possible extension are marked by a continuous and a dashed line, respectively; AM and DM: Ayrobera and Dubti manifestations respectively. Right: an example of MT data (MT station TDO010-118). Top: apparent resistivity curves; bottom: phase curves. Green dots mark the XY polarization data, red dots indicate the YX.

This is also the most probably cause of the higher electrical resistivity values detected by the magnetotelluric survey in the Ayrobera area with respect to Dubti (see below).

4. THE MAGNETIC SURVEY

Location of all the available GSE/Aquater magnetic data (Bekele, 2012) is shown in Fig. 3 (right). In order to reduce the effects of the stronger uneven spatial sampling, we have upward continued the residual magnetic anomaly up to 1 km above the topographic surface and obtained the map shown in Fig. 3. The 0 nT contour line (heavy black line) helps to individuate three main positive (high) domains labelled H1 – H2 and two negative (low) domains labelled L1 – L2. The L1 low is a long corridor trending NW-SE that separates the two high areas H1 and H2. We have traced the magnetic lineaments following the maxima of the total horizontal derivative of the terracing operator.

The anomaly pattern shown in the residual magnetic intensity anomaly map (Fig. 3) confirms the pattern enlightened by Bridges et al. (2012). The Tendaho magnetic field is characterized by an ~10 km wide linear negative magnetic anomaly that is flanked by two parallel, ~20-km-wide linear positive magnetic anomalies. The linear negative magnetic anomaly has been interpreted as an ~10 km region of dominantly normal-polarity intrusions and/or diking that follows the rift axis in the past ~0.8 m.y. of extension. On the contrary, the two linear positive magnetic anomalies have been interpreted as corresponding to reversed polarity zones due to basalts formed during the reverse Matuyama Chron (>0.78 Ma). However it is to note that mixed situations cannot be excluded, that is overlapping sills with different normal/reversed polarity may exist and probably are the standard. In this case the resultant anomaly may be positive or negative in function of the prevalent polarity in the basalts and also of their distance from the surface.

To gain insight in the magnetic anomaly pattern, we have modelled the simplest situation that can be expected, that is uniform basalts of normal or reverse-polarity, separated by vertical surfaces, extended down from the gravimetric bedrock surface modelled by 3D inversion of the gravimetric field. We have considered six profiles perpendicular to the graben axis. In Fig. 3 we show as example profile LM3. We have assigned to the sediments a susceptibility of 6 10-5 SI; to the bedrock a susceptibility of 0.023 SI and a remanent magnetism of 2.7 A/m, inclination -23°, declination 175° for the reverse polarity and of 2.7 A/m, inclination 16.8°, declination 1.46° for the normal polarity (from Bridges, 2011). Since the top surface of the basalts has been assumed as the "gravity bedrock surface" defined in par. 3 and obtained by inversion from the gravimetric data, the fit with the gravimetric signal is very good.

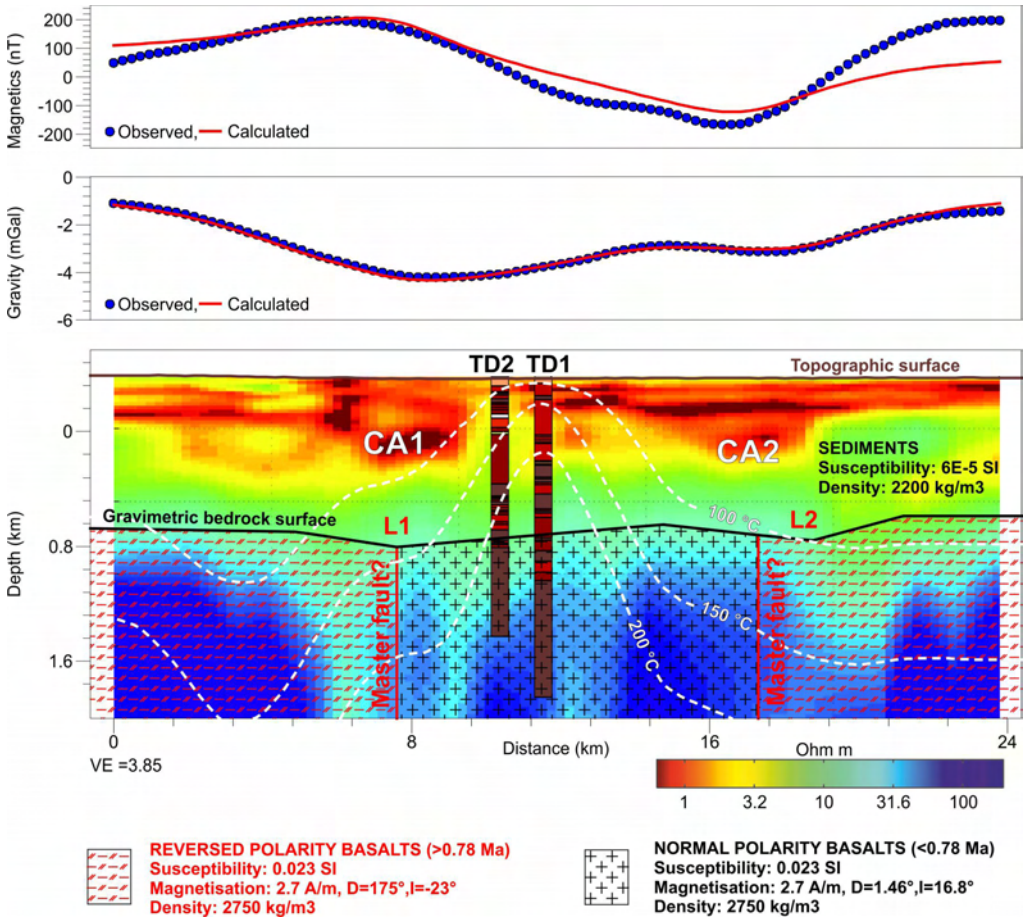

Figure 5 - 2D gravimetric and magnetic forward model along MT profile P9. Upper panel: observed and calculated residual magnetic intensity anomaly at 1 km above the topographic surface. Middle panel: observed and calculated residual free air anomaly at 1 km above the topographic surface. Lower panel: 2D simplified magnetic and gravimetric model superimposed to the electrical resistivity pseudo 2D model. The 100, 150, 200 °C isotherm contours are from the 3D temperature model of Stimac et al. (2014).

Then we have seek the vertical surface and the bottom plane surface that give the best fit with the magnetic data, assumed the magnetisation values indicated before. The fit of the magnetic data is quite good even with this simple model. It could be made better by varying the magnetisation and/or geometry parameters but it is just an useless exercise.

We have traced the horizontal location of the contact between the normal-reversed polarity zones in the map of Fig. 3 (left, marked by heavy black plus signs). The map shows that there is one main region where normal-polarity recent intrusions and/or diking focused. It is aligned along the central part of the graben, with the same trend. This ca. 10 km large stripe of dominantly intrusions/diking has been recording the past ~0.8 m.y. of extension in the graben. Note also a secondary stripe to the SW, not well defined by the data, that seem to converge with the main stripe in the southern part of the investigated area.

5. THE MAGNETOTELLURIC SURVEY

We processed the whole available MT dataset, i.e. the 229 MT stations acquired between 2007 and 2014, that comprise the new ARGeo MT and TDEM data (blue dots in Fig. 4). The MT stations are aligned along 16 profiles, as shown in Fig. 4, with an average separation of about 1 km. The distance between adjacent profiles is between 800 m and 4.5 km. Static shift corrections (Pellerin and Hohmann, 1990) were applied at the sites where TDEM data were available; otherwise the static shifts were estimated by spatial filtering techniques and/or considering it as free parameter in 2D modelling.

Magnetotelluric modelling has shown a widespread shallow conductor that is less continuous in the Ayrobera sector. The high conductivity is mainly related to the fine-grained sedimentary infill of the graben, with locally higher resistivity due to basaltic lavas and/or sills and coarser sediments.

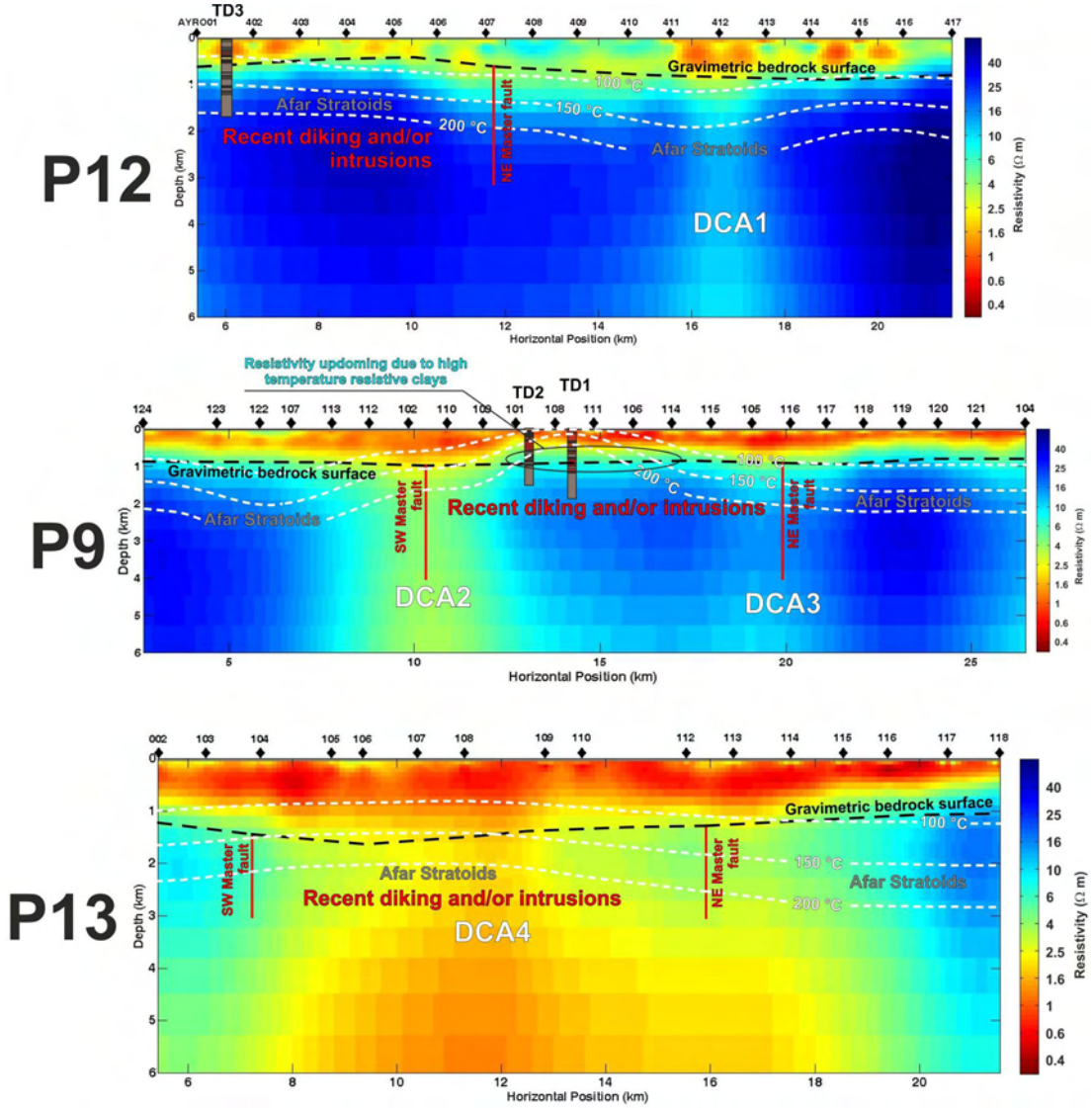

Figure 6 - 2D inverted models along MT profile P12, P9 and P13.

Therefore it is not possible to interpret everywhere up-doming of the shallow conductor as indicative of geothermal heating as usual (e.g. Muñoz, 2014). As stressed by Stimac et al. (2014), this indication can be considered plausible only relatively near thermal features where a thermal up-doming can be confirmed by independent constraints.

The shallow resistivity distribution can be enlightened by pseudo 2D sections made by 1D smooth models. They have higher resolution in the first 1 km depth than true 2D models and therefore can be used to map the basalts inter-beddings in the sediments. As example, we show here the model along profile P9, centred on the Dubti manifestations and crossing deep wells TD1 and TD2 (Fig. 5). The shallow low resistivity layer (resistivity less then ca. 3 Ohm m) shows two conductive anomalies labelled CA1 and CA2. These conductivity anomalies are located over the two master faults marked in red and flanking the region dominated by the recent (<0.78 Ma) activity. The two CA1 and CA2 conductivity anomalies can be related to i) abundant sedimentation processes following the focused erosion over the two master faults or to ii) more aggressive geothermal alteration processes due to abundant geothermal water coming from the two master faults, or to iii) a combination of the two previous processes. The isotherms of 100, 150, 200 °C (from the 3D temperature model of Stimac et al., 2014) traced over the mag, grav and resistivity models clearly indicate a higher heat flux density focused over the central region dominated by the recent (<0.78 Ma) normal-polarity intrusions and/or diking basalts. This model is also confirmed by the deep resistivity model presented by Lemma et al. (2014) over the same profile.

The distribution of resistivity at depth is enlightened by the true 2D models shown in Fig. 6 along profiles P12, P9 and P13 (see Fig. 4 for locations). Profile P9 shows two deep conductive anomalies (labelled DCA2 and DCA3) located in correspondence of the two edges of the anomalous stripe. DCA3 anomaly is weaker and not as well defined as DCA2. These features are quite similar to the model presented in Lemma et al. (2014).

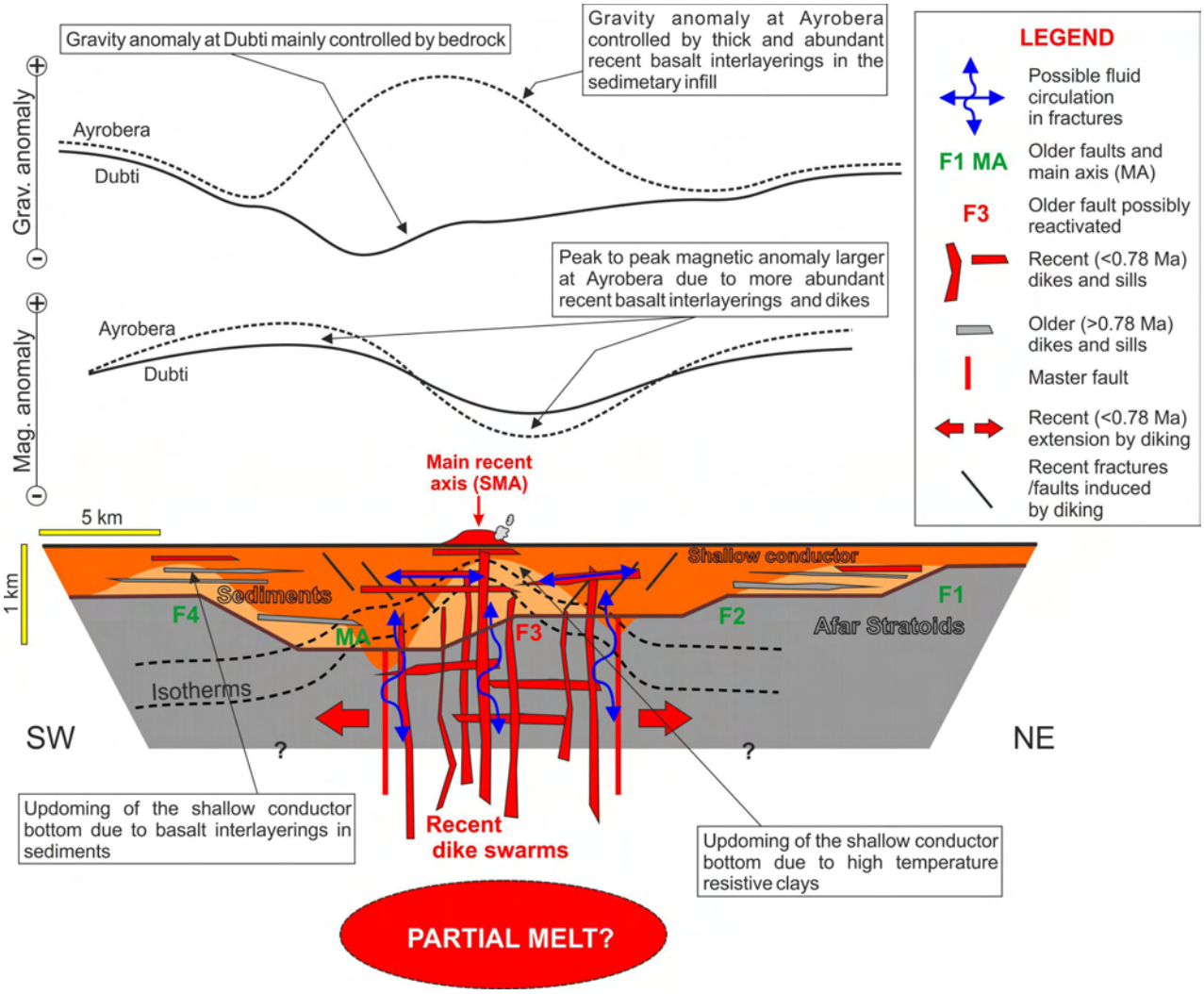

Figure 7 - Geophysical conceptual model (lower panel) across an ideal section from SW to NE crossing the Dubti manifestations and its typical geophysical signatures (upper panels). See the legend for symbols explanation.

These Authors have interpreted their corresponding anomaly DCA2 as an upper crustal fracture zone that lies above a 15 km wide area of partial melt. The melt fraction has been estimated of about 13% based on geochemical, borehole data, and bulk resistivity from the 2-D MT inversion model. The interpreted upper crustal partial melt may have been formed by either a magma intrusion from mantle sources or a large volume of continental crust that has been fluxed by a small amount of mantle melt and heat (Lemma et al., 2014). The inferred presence of a conductive fracture zone or fault with hydrothermal fluid and shallow heat sourcing magma reservoir has been also proposed by Desissa et al. (2013) for the close Dabbahu magmatic segment that has been active since 2005 and has experienced repeated magma intrusions. They interpreted, in a 2D MT profile, a 30 km wide conductive anomaly reaching down to about 35 km depth, as a large volume of magma of at least 500 km3 containing about 13% melt fraction. Profile P13 shows a wider and stronger deep conductive anomaly (labelled DCA4) approximately centred below the anomalous stripe of recent dikes/intrusions. This indicates that the conductive anomaly is shallower and more intense to the South of Dubti manifestations.

6. CONCLUSIONS

All the previous discussions have been summarized in a conceptual geophysical model shown in the sketch of Fig. 7, representing an ideal SW-NE section across the Dubti area. In summary, we can recognize the following features:

- Recent diking and sills (<0.78 Ma) intruded the older Afar Stratoids and the sediments above them along a NW-SE narrow stripe about 10 km large, causing fracturing/faulting and focused recent extension.
- Major dikes/sills volumes are concentrated in the Ayrobera sector.
- The magnetic negative anomaly marks normal polarity recent dikes/sills along the stripe both in the Ayrobera and Dubti sectors with decreasing intensity.
- The positive gravity anomaly in the Ayrobera sector is mainly due to abundant basalt interlayerings in the sediments. The gravity negative anomaly in the Dubti

Sector is mainly due to the Afar Stratoids bedrock variations.

• Sediments are marked by a shallow electrical conductor, with local variations due to basalt interlayerings and coarser components.

• High heat flux has focused along the narrow stripe of recent dike emplacement, possibly originated from deep heat sources with partial melt (deep electrical conductors).

• Enhanced heat flux induced local up-doming of the bottom of the shallow conductor due to conversion to high temperature resistive clays.

• The narrow stripe of diking induces faulting over a larger area above it.

• The highly faulted/fractured stripe facilitates deep/shallow fluid circulation and geothermal upflow.

REFERENCES

Abbate, E., Passerini, P., Zan, L., 1995. Strike-slip faults in a rift area: a transect in the Afar Triangle, East Africa. Tectonophysics, 241, 67-97

Abdurahman, S. A., 2011: Geochemistry of the Dubti wells and the Alalobeda hot springs. Proceedings Kenya Geothermal Conference.

Acocella, V., Abebe, B., Korme, T., Barberi, F., 2008. Structure of Tendaho Graben and Manda Hararo Rift: Implications for the evolution of the southern Red Sea propagator in Central Afar. Tectonics, 27

Acton, G.D., Tessema, A., Jackson, M., and Bilham, R., 2000, The tectonic and geomagnetic significance of paleomagnetic observations from volcanic rocks from central Afar, Africa. Earth and Planetary Science Letters, v. 180, p. 225-241.

Aquater, 1996. Tendaho Geothermal Project, Final Report, Volume 1: San Lorenzo in Campo,Italy, Aquater S.p.A., 324 p.

Battistelli, A., Amdeberhan, Y., Calore, C., Ferragina, C., Abatneh, W., 2002. Reservoir engineering assessment of Dubti geothermal field, Northern Tendaho Rift, Ethiopia. Geothermics 31, 381-406.

Bekele, B., 2012. Review and Reinterpretation of Geophysical Data of Tendaho Geothermal Field. The Geological Survey of Ethiopia, internal report.

Bekele, B., 2012. Review and Reinterpretation of Geophysical Data of Tendaho Geothermal Field. The Geological Survey of Ethiopia, internal report.

Bridges, D.L., 2011. A geological and geophysical study of the Tendaho Graben in the Afar depression, Ethiopia: insights into transitional continental rifting. PhD Thesis, Missouri University of Science and Technology.

Bridges, D.L., Mickus, K., Gao, S.S., Abdelsalam, M.G., Alemu, A.A., 2012. Magnetic stripes of a transitional continental rift in Afar. Geology, doi:10.1130/G32697.1

Desissa, M., Johnson, N.E.,Whaler K.A., Hautot S., Fisseha S., Dawes G.J.K, 2013. A mantle magma reservoir beneath an incipient mid-ocean ridge in Afar, Ethiopia. Nature Geoscience, 6, 861-865, DOI: 10.1038/NGEO01925

Didana, Y.L., Thiel, S., Heinson, G., 2015. Three dimensional conductivity model of the Tendaho High Enthalpy Geothermal Field, NE Ethiopia. Journal of Volcanology and Geothermal Research, 290, 53–62

Kidane, T., Courtillot, V., Manighetti, I., Audin, L., Lahitte, P., Quidelleur, X., Gillot, P.-Y., Gallet,Y., Carlut, J., and Haile, T., 2003. New paleomagnetic and geochronologic results from Ethiopian Afar: Block rotations linked to rift overlap and propogation and determination of a ~2 Ma reference pole for stable Africa. Journal of Geophysical Research, v. 108, p. 2102.

Lemma, Y., Hailu, A., Desissa, M., and Kalberkamp, U., 2010, Intergrated geophysical surveys to characterize Tendaho Geothermal Field in north eastern Ethiopia: Proceedings World Geothermal Congress: Bali, Indonesia.

Lemma, Y., Thiel, S. and Heinson, G, 2014. Magnetotelluric imaging of upper crustal partial melt at Tendaho graben in Afar, Ethiopia. Geophys. Res. Lett., 41, 3089–3095, doi:10.1002/2014GL060000.

Stimac, J., E. Armadillo, S. Kebede, M. Zemedkun, Y. Kebede, A. Teclu, D. Rizzello, P. E. Mandeno, 2014. Integration and Modeling of Geoscience Data from the Tendaho Geothermal Area, Afar Rift, Ethiopia. Proceedings 5th African Rift geothermal Conference Arusha, Tanzania.

Teklemariam Zemedkun, M., 2011. Overview of Geothermal Resource Exploration and Development in the East African Rift System. Proceedings, Short Course VI on Exploration for Geothermal Resources, Lake Bogoria, Kenya.